



**HAL**  
open science

# Vlasov simulations of ultrafast electron dynamics and transport in thin metal films

Giovanni Manfredi, Paul-Antoine Hervieux

► **To cite this version:**

Giovanni Manfredi, Paul-Antoine Hervieux. Vlasov simulations of ultrafast electron dynamics and transport in thin metal films. *Physical Review B*, 2004, 70 (20), pp.201402. 10.1103/PhysRevB.70.201402 . hal-04789753

**HAL Id: hal-04789753**

**<https://hal.science/hal-04789753v1>**

Submitted on 21 Nov 2024

**HAL** is a multi-disciplinary open access archive for the deposit and dissemination of scientific research documents, whether they are published or not. The documents may come from teaching and research institutions in France or abroad, or from public or private research centers.

L'archive ouverte pluridisciplinaire **HAL**, est destinée au dépôt et à la diffusion de documents scientifiques de niveau recherche, publiés ou non, émanant des établissements d'enseignement et de recherche français ou étrangers, des laboratoires publics ou privés.

# Vlasov Simulations of Ultrafast Electron Dynamics and Transport in Thin Metal Films

G. Manfredi<sup>1</sup> and P.-A. Hervieux<sup>2</sup>

<sup>1</sup>*Laboratoire de Physique des Milieux Ionisés et Applications,*

*CNRS - Université H. Poincaré, BP 239, F-54506 Vandoeuvre-les-Nancy, France*

<sup>2</sup>*Institut de Physique et Chimie des Matériaux de Strasbourg, GONLO, BP 43, F-67034 Strasbourg, France*

(Dated: February 24, 2005)

The ultrafast dynamics of electrons and ions in thin metal films has been investigated using a semi-classical model based on self-consistent Vlasov simulations. The Vlasov equation is solved using a very accurate Eulerian scheme that preserves the fermionic character of the electron distribution for all times. With this technique, the electronic transport and thermalization are studied on a time scale of over 150 plasmon cycles. Our results demonstrate that heat transport occurs at a velocity close to the Fermi velocity, in agreement with experimental measurements in thin gold films. We also show that: (i) internal electron thermalization can be achieved without including any binary electron-electron collisions and (ii) nonequilibrium electrons begin to interact with the lattice well before the internal electron thermalization is completed. These effects are considerably enhanced by the interaction of nonequilibrium electrons with the film surfaces.

Understanding the relaxation processes of an electron gas confined in a nanosized structure is a matter of great importance in materials science, both for fundamental studies and technological applications. Although the physical properties of the bulk matter are rather well understood, the ion and electron dynamics in finite-size nanoscale systems are believed to display novel and unexpected features, due to the presence of interfaces. The aim of this Letter is to provide a deeper insight into the properties of electron thermalization and transport in typical finite-size systems, such as thin metal films.

It is nowadays possible, by means of ultrafast spectroscopy techniques, to assess the femtosecond dynamics of an electron gas confined in metallic thin films<sup>1-6</sup> or nanoparticles<sup>6-8</sup>, so that theoretical predictions can be directly compared to experimental measurements. In a typical femtosecond pump-probe experiment the following schematic scenario is generally assumed: first, the electrons absorb quasi-instantaneously the laser energy via interband and/or intraband transitions. During this process, the ionic background remains frozen and the electron distribution is non-thermal. On a femtosecond time scale, the injected energy is redistributed among the electrons via electron-electron collisions, leading to the so-called internal electron thermalization. Electron-lattice (“external”) thermalization was generally supposed to occur on longer time scales. However, the results of Refs.<sup>5,9</sup> on thin gold films have shown that nonequilibrium electrons start interacting with the lattice earlier than expected, so that a clear separation between internal and external relaxation is not entirely pertinent. Other experiments have measured the properties of heat transport in thin gold films<sup>1,2</sup>, showing that it is not a diffusive process (Brownian motion), but rather a ballistic one (motion at constant velocity). These works demonstrated that heat transport occurs on a femtosecond time scale and involves nonequilibrium electrons travelling at a velocity close to the Fermi velocity of the metal. In the present paper, we shall provide numerical evidence

in support of the above experimental findings.

In order to model and interpret experimental results obtained with thin metallic films, ab-initio methods can hardly be employed, as they involve prohibitive computational times. Several authors<sup>3,5,9</sup> have resorted to phenomenological Boltzmann-type equations that provide the time evolution of the electron occupation number in the bulk metal, but this approach neglects the effect of spatial inhomogeneities and surfaces. A possible alternative relies on the use of microscopic kinetic methods, originally developed in nuclear and plasma physics, and applied more recently to metal clusters<sup>10</sup>. In these models, the valence electrons are assimilated to an inhomogeneous electron plasma. Here, we shall focus our attention on alkali metals, and more specifically sodium films, for which the influence of the core electrons can be neglected; such systems can be realized experimentally<sup>11</sup>. The semi-classical electron dynamics can be described in phase space by the Vlasov equation, coupled self-consistently to Poisson’s equation.

The numerical resolution of the Vlasov equation is usually performed by particle-in-cell (PIC) methods, which approximate the distribution function by a finite number of test particles<sup>10</sup>. However, the numerical noise inherent to this method is too large to allow a precise description of the distribution function in phase space. Further, due to the finite number of particles used, PIC methods inevitably introduce some amount of random noise in the Vlasov dynamics, which drives the system towards classical Maxwell-Boltzmann thermalization. Therefore, the fermionic character of the electrons is not preserved during time evolution<sup>12</sup>, which constitutes a major drawback for any PIC method. The accuracy of PIC simulations can be somewhat improved by using finite-size particles<sup>13</sup> or by introducing ad-hoc collision operators<sup>14</sup>. Nevertheless, Maxwell-Boltzmann thermalization is still observed after some time. In addition, these corrections make it difficult to separate the mean-field Vlasov dynamics from the effect of such ad-hoc terms.

On the contrary, Eulerian codes<sup>15</sup> rely on the solution of the Vlasov equation on a regular mesh in the phase space  $(x, v)$ . They generally achieve finer resolution and display better convergence and stability properties than the corresponding PIC codes. As they are not based on discrete particles, Eulerian codes do not introduce any statistical noise liable to drive the electron gas towards Boltzmann equilibrium. Here, we shall employ a recently developed Eulerian scheme<sup>16</sup>, which is capable of preserving the fermionic character of the electron distribution *exactly and for all times*. Thanks to this numerical technique, we have been able to obtain clean and meaningful information on the electron and ion thermalization in a thin metal film.

In the forthcoming simulations, time is normalized in units of the inverse plasmon frequency  $\omega_{pe}^{-1}$ , velocity in units of the Fermi speed  $v_F$ , and length in units of  $L_F = v_F/\omega_{pe}$ . For alkali metals we have  $L_F = 0.59 (r_s/a_0)^{1/2} \text{ \AA}$ ,  $\omega_{pe}^{-1} = 1.33 \times 10^{-2} (r_s/a_0)^{3/2} \text{ fs}$ ,  $E_F = 50.11 (r_s/a_0)^{-2} \text{ eV}$  and  $T_F = 5.82 \times 10^5 (r_s/a_0)^{-2} \text{ K}$ , where  $r_s$  is the Wigner-Seitz radius. For sodium,  $r_s = 4a_0$  with  $a_0 = 0.529 \text{ \AA}$ . The electron and ion plasmon period are, respectively,  $0.67 \text{ fs}$  ( $\approx 6.28 \omega_{pe}^{-1}$ ) and  $137.68 \text{ fs}$  ( $\approx 1300 \omega_{pe}^{-1}$ ). In the following,  $m_e$  and  $m_i$  are the electron and ion mass and  $e$  denotes the absolute electron charge.

We consider a system of electrons interacting via a Coulomb potential and confined within a slab of thickness  $L$ . The ion background is represented by a positive charge density with soft edges,  $\rho_i(x) \equiv en_i(x) = e\bar{n}_i [1 + \exp((|x| - L/2)/\sigma_i)]^{-1}$ , where  $\bar{n}_i = 3/(4\pi r_s^3)$  is the ion density of the bulk metal and  $\sigma_i$  a diffuseness parameter<sup>10</sup>. In this jellium model, the self-consistent electrostatic potential depends only on the coordinate normal to the surface (here noted  $x$ ). Thus, the motion of an electron parallel to the surface of the film is completely decoupled from the motion normal to the surface, and a one-dimensional (1D) model can be adopted.

Initially, electrons and ions are assumed to be at thermal equilibrium with the same temperature. The electrons are treated by a semi-classical Thomas-Fermi approach, their energy distribution being a 3D Fermi-Dirac function with temperature  $T_e$ . The 1D distribution is obtained by integrating over the velocity variables parallel to the surface. For an equilibrium at finite electron temperature, the 1D Fermi-Dirac distribution reads as

$$f_e(x, v, 0) = \frac{3}{4} \frac{\bar{n}_i}{v_F} \frac{T_e}{T_F} \ln \left[ 1 + \exp \left( -\frac{\epsilon(x, v) - \mu}{k_B T_e} \right) \right], \quad (1)$$

where  $\epsilon(x, v) = m_e v^2/2 - e\phi(x)$  is the single-particle energy and  $\mu$  is the chemical potential. At  $T_e = 0$ , the above expression becomes linear in  $\epsilon$ . The ions are classical and initially obey a Maxwell-Boltzmann distribution with density  $n_i(x)$  and temperature  $T_i$ .

The calculation of the ground state is thus reduced to the resolution of Poisson's equation

$$\frac{d^2\phi}{dx^2} = \frac{e}{\epsilon_0} [n_e(x) - n_i(x)], \quad (2)$$

with  $n_e = \int f_e dv$ . The chemical potential  $\mu$  is determined by requiring global charge neutrality:  $\int n_e dx = \int n_i dx$ . We have not included any exchange-correlation energy in the model, although this could be done relatively easily within the local-density approximation<sup>18</sup>. These effects are of minor importance and should not change the conclusions of the present work. The above nonlinear Poisson equation is solved with an iterative method that yields the self-consistent potential  $\phi(x)$  and the corresponding electron distribution  $f_e(x, v, 0)$ .

We consider situations where no linear momentum is transferred parallel to the plane of the surface (i.e. only excitations with  $q_{\parallel} = 0$  are taken into account). This situation corresponds to the excitation of the slab with optical pulses<sup>17</sup> and also to the response to a uniform electric field oriented normal to the surface. The dispersion relation of the slab collective modes is given by the well-known expression<sup>18</sup>:  $\omega_{\pm}(q_{\parallel}) = \omega_{pe} \sqrt{(1 \mp e^{-q_{\parallel}L})/2}$ . For  $q_{\parallel} = 0$ , only longitudinal modes (volume plasmon with  $\omega = \omega_{pe}$ ) can be excited.

The evolution of the electron and ion distribution functions  $f_e$  and  $f_i$  is governed by the Vlasov equations

$$\frac{\partial f_{e,i}}{\partial t} + v \frac{\partial f_{e,i}}{\partial x} - \frac{q_{e,i}}{m_{e,i}} \frac{\partial \phi}{\partial x} \frac{\partial f_{e,i}}{\partial v} = 0 \quad (3)$$

where  $q_e = -e$ ,  $q_i = +Ze$  (we consider only monovalent metals,  $Z = 1$ ). The ion and electron Vlasov equations are coupled via the electrostatic potential, obtained self-consistently at each instant from Poisson's equation (2).

The stability properties of the numerical technique employed here have been tested by preparing the system in its ground state and letting it evolve self-consistently without any perturbation. By definition, the ground state is a stationary solution of the Vlasov-Poisson system and should remain stable under the time evolution. However, PIC codes show a rather quick deterioration of the Fermi-Dirac ground state, which relaxes to a Boltzmann distribution in a few ( $\approx 13$ ) electron plasmon cycles<sup>13,14</sup>. With our Eulerian code, no departure from the Fermi-Dirac equilibrium can be detected for times as long as  $\omega_{pe}t = 1000$ , corresponding to more than 150 plasmon cycles. The initial and final energy distributions (obtained by integrating  $f_e$  over different energy surfaces) are shown in Fig. 1 (thin solid lines) and are virtually indistinguishable on the scale of the figure. The total energy is conserved within an error of less than 0.05%.

We now turn to the case where a perturbation is imposed on the initial equilibrium in order to excite the electron dynamics. All simulations were performed using realistic parameters: an initial temperature  $T_e = T_i = 0.008 T_F \simeq 300 \text{ K}$ , a diffuseness parameter  $\sigma_i = 0.3 L_F$ <sup>18</sup>, and a slab of thickness  $L = 100 L_F \simeq 118 \text{ \AA}$ <sup>17</sup>. In order to assess the impact of the ion dynamics on the electron thermalization, two sets of simulations were performed: with fixed ions ( $m_i \rightarrow \infty$ ) and with mobile sodium ions ( $m_i = 42228 m_e$ ). The thin film is excited by imposing a constant velocity shift  $\delta v$  to the initial electron distribution. In this way, an amount of energy  $E^* = L\delta v^2/2$  (in

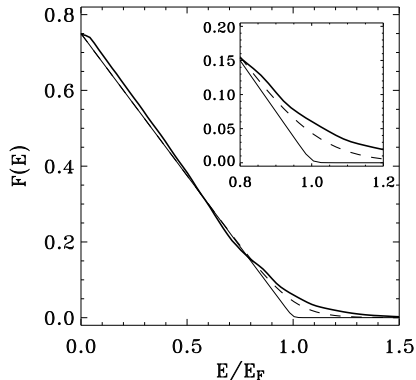


FIG. 1: Electron energy distribution at  $t = 0$  (thin solid line) and  $\omega_{pe}t = 1000$  (thick solid line) for fixed ions. The dashed line is a Fermi-Dirac function with  $T_e = 0.084 T_F$ . The inset shows a zoom around the Fermi surface.

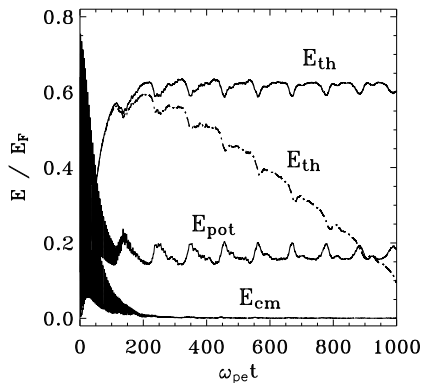


FIG. 2: Time evolution of several energy quantities. Solid lines: fixed ions; dot-dashed line: mobile ions.

normalized units) is injected into the system. We have adjusted the value of  $\delta v = 0.08v_F$  in order to have  $E^* = 2$  eV, which is typical for experiments using femtosecond laser pulses<sup>1,2</sup>. The resulting energy distribution function at  $\omega_{pe}t = 1000$  is displayed in Fig. 1 (thick solid line) for the fixed-ions case. For the sake of comparison, a Fermi-Dirac distribution with temperature  $T_e^{\text{final}} = 0.084 T_F$  is also plotted on the same graph (dashed line). This final temperature is obtained from the electron thermal energy (see next paragraph for its definition) corresponding to the electron distribution at  $\omega_{pe}t = 1000$ . Clearly, the electron gas has evolved towards a new quasi-equilibrium state characterized by a distribution function close to a Fermi-Dirac function with a temperature higher than the ground state.

In order to investigate the approach to such a quasi-equilibrium state, the time evolution of some pertinent energy quantities was analyzed. The total energy of the electron gas is given by:  $E_{\text{tot}} = E_{\text{kin}} + E_{\text{pot}}$ . Further, the kinetic energy can be split into three parts: (i) the kinetic energy of the center of mass:  $E_{\text{cm}} = \frac{1}{2} \int \frac{j_e^2(x)}{n_e(x)} dx$  (where  $j_e = \int v f_e dv$  is the electron current); (ii) the Thomas-

Fermi energy (energy of the equivalent zero-temperature state with same density):  $E_{\text{TF}} = \frac{1}{10} \int n_e(x)^{5/3} dx$ ; and (iii) the thermal energy:  $E_{\text{th}} = E_{\text{kin}} - E_{\text{cm}} - E_{\text{TF}}$ . In Fig. 2, the time evolution of  $E_{\text{th}}$ ,  $E_{\text{pot}}$  and  $E_{\text{cm}}$  is shown for two runs with fixed (solid lines) and mobile (dashed line) ions. For clarity, only  $E_{\text{pot}}$  and  $E_{\text{cm}}$  corresponding to the fixed-ion case are depicted on the figure, as they are almost identical to those observed in the mobile-ion simulation (apart from some weak damping).

Several phases can be identified in the time evolution. An initial phase corresponds to the damped collective oscillations of the electron gas occurring at the plasmon frequency  $\omega_{pe}$ . These fast oscillations are observed in the behavior of  $E_{\text{pot}}$  and  $E_{\text{cm}}$  up to  $\omega_{pe}t \simeq 200$ . At this time, the center-of-mass energy is almost entirely converted into thermal energy (kinetic energy around the Fermi surface). The Thomas-Fermi energy (not shown on the figure) remains almost unchanged during the entire run. After saturation of the thermal energy at  $\omega_{pe}t \simeq 200$ , a slowly oscillating behavior appears, with period  $\approx 100\omega_{pe}^{-1}$ . This period is roughly equal to the time of flight of out-of-equilibrium electrons travelling through the slab at a velocity close to the Fermi velocity of the metal. It corresponds to particles colliding with either surface and being reflected back. Indeed, we have verified that the oscillation period doubles when considering a film that is twice as thick as the present one. The persistence of such oscillations indicates that the thermalization process observed in Fig. 1 is not quite complete by the end of the run. These results show that electron-surface interactions play an important role in the thermalization process. This is not unexpected, since the thickness of the slab is smaller than the electron mean free path, which for bulk sodium, is equal to  $340 \text{ \AA}$ <sup>19</sup>.

Similar oscillations were recently measured in transient reflection experiments on thin gold films, and it was observed that the oscillation period scales linearly with the thickness of the film<sup>20</sup>. The explanation provided by the authors (electrons bouncing back and forth against the film surfaces at a speed close to  $v_F$ ) is basically identical to our interpretation of the present numerical results.

Further, comparing the evolution of  $E_{\text{th}}$  for the runs with mobile and fixed ions, it appears that energy exchanges between the electrons and the lattice occur much faster ( $\omega_{pe}t = 150$ , corresponding to 16 fs) than in the bulk metal, and well before complete internal electron thermalization has occurred. However, these early energy exchanges are localized at the film surfaces (see Fig. 3): complete electron-ion thermalization over the entire film will take much longer times.

The fine resolution of our Eulerian code allows us to investigate in detail the microscopic electron and ion dynamics in the relevant phase space. The electron phase space dynamics is shown in Fig. 3 (left frames), where  $f_e(x, v, t)$  is displayed for  $\omega_{pe}t = 0, 50$  and  $100$ . It is clear that the perturbation propagates coherently from surface to surface with a speed  $v_0 \simeq 0.85v_F$ , slightly smaller than the Fermi velocity. Coherent structures (vortices)

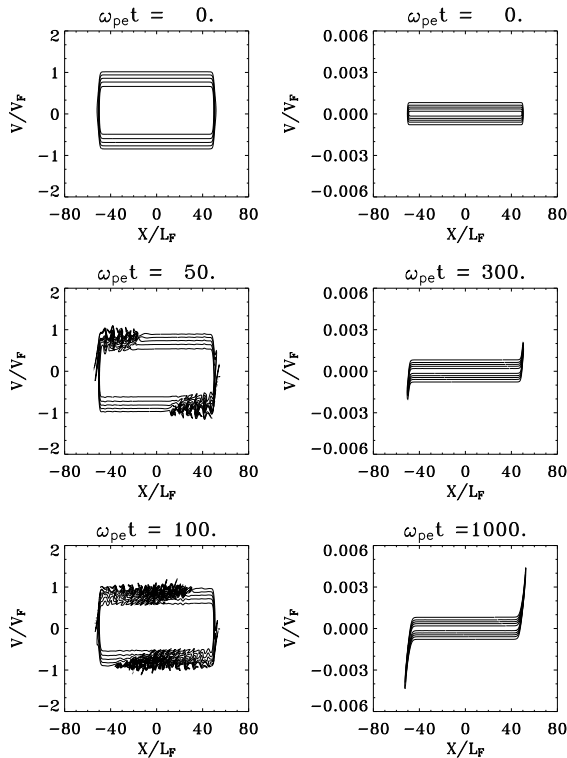


FIG. 3: Electron (left) and ion (right) phase space portraits. Note that the times are *not* the same for ions and electrons.

are indeed observed around the phase space region with velocity  $v_0$ . These structures correspond to nonequilibrium electrons being trapped in the propagating wave and are known to appear in wave-particle interactions in classical plasmas<sup>21</sup>. These results demonstrate beyond any doubt that heat transport is ballistic and occurs at a velocity close to  $v_F$ , in agreement with experimental measurements in thin gold films<sup>1,2</sup>. When the perturbation reaches the opposite surface ( $\omega_{pe}t \simeq 120$ ), it is reflected back and interacts with the rest of the nonequi-

librium electrons, thus inducing a loss of the coherence (vortices are destroyed). After several collisions with the surfaces, most of the nonequilibrium electrons are spread in a region around the Fermi surface, leading to a high-temperature quasi-equilibrium state with a Fermi-Dirac energy distribution, as was shown in Fig. 1. Nevertheless, such mean-field thermalization is not quite complete, as the final energy distribution is not exactly a Fermi-Dirac one (Fig. 1) and some periodic oscillations still persist (Fig. 2).

The related ion phase space dynamics is depicted in Fig. 3 (right frames), where  $f_i(x, v, t)$  is plotted for several instants. We note that the electron-ion energy exchange is localized at the surfaces of the slab<sup>7</sup>, where the ions are accelerated to velocities much larger than their initial thermal speed  $\sqrt{k_B T_i / m_i} \simeq 3 \times 10^{-4} v_F$ . The energy necessary to accelerate the ions to such velocities is mainly extracted from the electron kinetic energy, as shown in Fig. 2, where  $E_{th}$  decreases significantly for the simulation with mobile ions. We stress that the electron-ion coupling observed here is due to the mean field alone via Poisson's equation.

In summary, the present results provide new insights into the processes of electron thermalization in confined metallic structures, with particular emphasis on the role of surfaces. Thanks to accurate Vlasov simulations, we have shown that electron thermalization can be achieved, to a large extent, even in the absence of binary electron-electron collisions. This mean-field quasi-thermalization is due to nonequilibrium electrons bouncing back and forth against the film surfaces at a speed close to the Fermi velocity of the metal. Further, nonequilibrium electrons begin to interact with the ion lattice well before internal electron thermalization is completed, so that a significant fraction of the electron thermal energy is transferred very early to the lattice.

We thank P. Bertrand, J.-Y. Bigot and F. Huot for helpful discussions.

<sup>1</sup> S. D. Brorson, J. G. Fujimoto, and E. P. Ippen, Phys. Rev. Lett. **59**, 1962 (1987).  
<sup>2</sup> C. Suárez, W. E. Bron, and T. Juhasz, Phys. Rev. Lett. **75**, 4536 (1995).  
<sup>3</sup> R. H. M. Groeneveld, R. Sprik, and A. Lagendijk, Phys. Rev. B **51**, 11433 (1995).  
<sup>4</sup> G. L. Eesley, Phys. Rev. Lett. **51**, 2140 (1983).  
<sup>5</sup> C.-K. Sun et al., Phys. Rev. B **50**, 15337 (1994).  
<sup>6</sup> J.-Y. Bigot, V. Halté, J.-C. Merle, and A. Daunois, Chem. Phys. **251**, 181 (2000).  
<sup>7</sup> M. Nisoli et al., Phys. Rev. Lett. **78**, 3575 (1997).  
<sup>8</sup> C. Voisin et al., Phys. Rev. Lett. **85**, 2200 (2000).  
<sup>9</sup> W. S. Fann et al., Phys. Rev. B **46**, 13592 (1992).  
<sup>10</sup> F. Calvayrac et al., Phys. Rep. **337**, 493 (2000).  
<sup>11</sup> M. Breitholtz et al., Phys. Rev. B **64**, 073301 (2001).  
<sup>12</sup> K. Morawetz and R. Walke, Physica A **330**, 469 (2003).  
<sup>13</sup> A. Doms et al., Ann. Phys. (Leipz.) **6**, 468 (1997).

<sup>14</sup> A. Doms, P.-G. Reinhard, and E. Suraud, Ann. Phys. (N.Y.) **260**, 171 (1997).  
<sup>15</sup> C. Z. Cheng and G. Knorr, J. Comput. Phys. **22**, 330 (1976).  
<sup>16</sup> F. Filbet, E. Sonnendrucker, and P. Bertrand, J. Comput. Phys. **172**, 166 (2001).  
<sup>17</sup> M. Anderegg, Phys. Rev. Lett. **27**, 1575 (1971).  
<sup>18</sup> A. Liebsch, *Electronic Excitations at Metal Surfaces* (Plenum Press, New York, 1997).  
<sup>19</sup> U. Kreibitz and M. Vollmer, *Optical Properties of Metal Clusters*, Springer-Verlag, Inc., New York, 1995.  
<sup>20</sup> X. Liu, R. Stock, and W. Rudolph, CLEO/IQEC and PhAST Technical Digest on CDROM (The Optical Society of America, Washington, DC, 2004), IWA4.  
<sup>21</sup> G. Manfredi, Phys. Rev. Lett. **79**, 2815 (1997).